THE EFFECT OF AN OBSTACLE IN THE ABLATION PLASMA ON THE ELECTRICALPROPERTIES OF THE OXIDE THIN FILMS

FLORIN GHERENDI*, MAGDALENA NISTOR, NICOLAE B. MANDACHE
National Institute for Lasers, Plasma and Radiation Physics, L.22,
P.O.Box MG-32, 077125, Bucharest-Magurele, Romania
*florin.gherendi@infim.ro

ABSTRACT

The pulsed electron beam ablation deposition method (PED) was used for growing In_2O_3 and ZnO transparent oxide thin films with a metal strip placed inside the ablation plasma plume as mechanical obstacle. Pure oxygen was used as working gas. The influence of the obstacle on the properties of the ablation plasma was studied with an ion probe and by resistivity measurements on the deposited thin films respectively. A 16 times reduction of the ion density was evidenced by the ion probe behind the obstacle. The film resistivity varies from $2 \cdot 10^{3}$ Ω·cm in the obstacle shadow to $3 \cdot 10^{-4}$ Ω·cm in the adjacent (non-shadowed) regions for In_2O_3 films, while for ZnO films the variation is from 0.6 Ω·cm to $6 \cdot 10^{-3}$ Ω·cm. The increase of the resistivity of the film grown behind the obstacle as compared to the adjacent regions was explained by a reduction of the concentration of oxygen vacancies due to a relatively larger contribution of the oxygen incorporated in the film from the working gas in the lower plasma density region behind the obstacle. The smaller variation in the case of ZnO target was explained by the increased scattering of Zn ions behind the obstacle in comparison to the In ions, due to their smaller mass.

1. INTRODUCTION

In recent years transparent conducting oxide thin films as indium oxide (In_2O_3) and zinc oxide (ZnO) were widely studied as n-type device materials in transparent thin film transistors due to their excellent optical transmission in visible region, tunability of the electrical properties and chemical stability [1, 2, 3, 4]. The high demand from the consumers for high resolution and large panel displays leads to the necessity of low-cost fabrication of such transistors. One approach is to obtain during a single deposition process a fine spatially tuning of the electrical and optical properties of the oxide film such as self-assembled transparent transistors can be fabricated [5]. This can be accomplished by inserting an obstacle in an ablation plasma plume, leading to a local modification of the electrical film properties [5, 6].

PED is an ablation deposition method [7, 8] similar to the pulsed laser deposition (PLD), but using a pulsed electron beam instead of the laser beam for ablating the target. The main advantage of these methods is that the stoichiometry of the bulk target is preserved in deposited thin films. As an example, stoichiometric, dense, smooth and epitaxial ZnO and In_2O_3 thin films have been grown by PED with various electrical and optical properties [7-10].

Previously, studies with obstacles in ablation plasma were carried out for PLD [11], with the purpose of improving the film surface quality by reducing the quantity of droplets at the film surface, but without exploring in detail the film properties under obstacle. In this work, the thin films grown by PED are smooth, thus the aim is to investigate the manner in which the presence of an obstacle in the ablation plasma plume influences the electrical properties of semiconducting oxide thin films during a single deposition process

2. EXPERIMENTAL SETUP

The PED device, described in detail in previous paper [7, 8], generates a 100 ns pulsed electron beam in a channel-spark discharge. The electron source consists of a hollow cathode, a dielectric capillary tube (6 mm diameter and 110 mm length) and a vacuum chamber as grounded anode. The target-substrate distance is 40 mm and the capillary tube is set at an angle of 45°.

In the present work, In_2O_3 and ZnO transparent oxide thin films were grown by PED in $1.3 \cdot 10^{-2}$ mbar pure oxygen, at a -14kV working voltage and at room temperature on glass substrates. A metal (stainless steel) strip 10 mm wide is placed inside the ablation plasma plume

as obstacle, at a distance of 23 mm from the ablation target. Either an ion probe or a substrate was placed at 17 mm behind the obstacle. The film growth setup is schematically presented in figure 1.

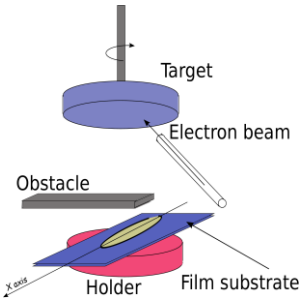

Fig. 1: Experimental setup for the film growth with obstacle

Resistivity measurements were carried out at room temperature on the thin films along the x-axis shown in fig. 1.
In the case of ion probe measurements (figure 2), the probe is placed at the substrate position.

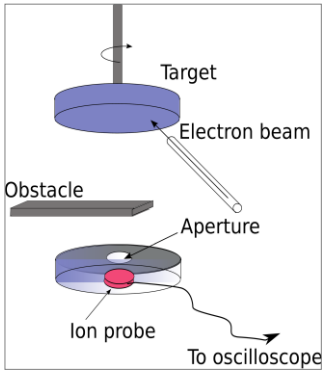

Fig 2: Setup for ion probe measurements with obstacle

The disc-shaped 4 mm diameter ion probe was enclosed in a metal cylinder having a 2 mm diameter aperture with the role of separating the expanding ablation plume from the background plasma, associated to the discharge which generates the pulsed electron beam. [7, 12].

3. RESULTS

A typical -14 kV high voltage signal is shown in Fig. 3a. The synchronized ion probe signals of the In_2O_3 ablation plasma for a working pressure of $1.3 \cdot 10^{-2}$ mbar oxygen, recorded with and without obstacle, are presented in figure 3b. The ion probe was biased -30 V for repelling the electrons.
All probe signals start with a negative peak due to the fast electrons (which could not be stopped by the 30V reverse bias). These electrons are originating from the pulsed electron beam, being reflected/scattered on the target at large angles, and they are synchronized with the high voltage fall, as it can be seen in figure 3. The ion pulse has a peak occurring at 5.04 μs from the discharge voltage fall time without obstacle, and 5.22 μs with obstacle, respectively. This slight difference could be attributed to the time needed for the ions to bypass the obstacle.

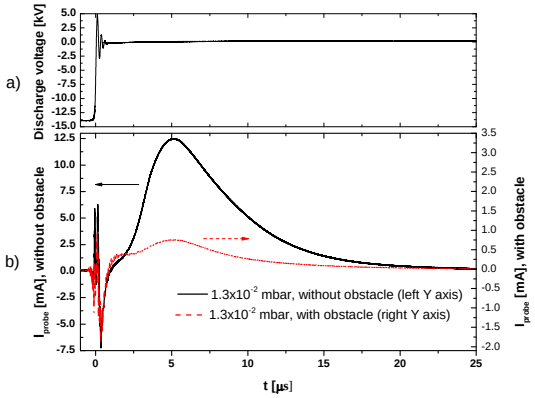

Fig. 3:a) Typical PED high voltage trace b) Ion probe signals with (straight line) and without obstacle (dotted line), at a -30V probe bias

The mean ion energy determined by the time-of-flight method was ~37.5 eV without obstacle and ~35 eV with obstacle. The area under the ion current waveform is a measure of the total number of ions reaching the probe. There is a ratio of ~16 between the areas of the ion current waveforms without obstacle and with obstacle at the same pressure.
In_2O_3 and ZnO films were grown on glass substrates under same conditions as those used for the ion probe measurements. The comparative film thicknesses for In_2O_3 and ZnO, measured with spatial resolution using a profilometer, are presented in figure 4.

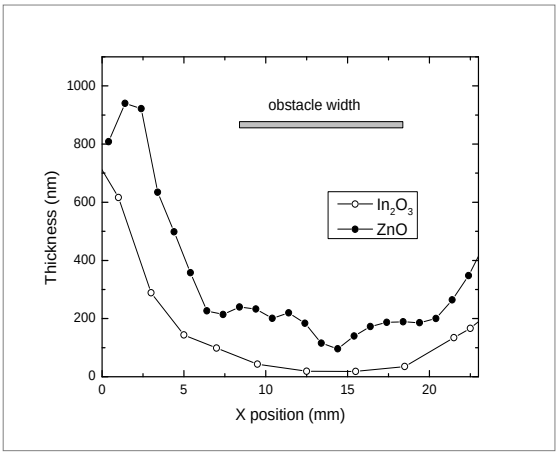

Fig 4: Comparative thickness profile of the In_2O_3 and ZnO films grown with obstacle

The thickness measurements indicate a minimum In_2O_3 film thickness of 20 nm in the middle of the obstacle shadow, 40 times smaller than the 800 nm thickness in the adjacent regions of the film. As it can be seen in figure 4, the ZnO film at the same ambient gas pressure and deposition time is significantly thicker behind the obstacle as compared to the In_2O_3 film (min ~100nm vs. min. ~20nm), even if they have approximately the same thickness in the non-shadowed wings. We explain this by the smaller mass of Zn ions (~65 a.m.u. as compared to ~118 a.m.u. for In), which determines a smaller mean free path in the ambient gas [13], otherwise said a more significant scattering of the Zn ions by the working gas. More scattering is leading to a higher density of the Zn ions behind the obstacle, therefore a greater thickness of the film grown in this region in comparison with the In_2O_3 film.

Both ZnO and In_2O_3 films have a noticeable build-up region in the vicinity of the obstacle shadow. Indeed, films grown in separate experiments without obstacle at the same pressure and high voltage have a thickness of ~400 nm, compared to the ~800 nm seen in figure 4. Taking into account the build-up thickness, which approximately doubles the thickness of the film grown without obstacle, an In_2O_3 film would be in fact only 20 times thinner behind the obstacle, matching the ~16 times reduction of the plasma density indicated by the ion probe. The remaining difference could be explained by the fact that the ion probe gives no information about the neutral species in the plasma.

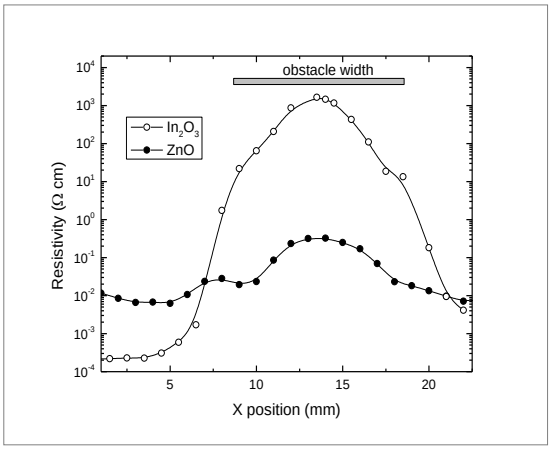

Fig 5: Comparative resistivity profile of the In_2O_3 and ZnO films grown with obstacle

The electrical properties of the thin films grown on glass substrate in the obstacle shadow at room temperature and $1.3 \cdot 10^{-2}$ mbar oxygen were investigated in comparison with the properties of the non-shadowed film regions. The resistivity of the films was measured with one-dimensional spatial resolution across the obstacle shadow, using electrical probes [5, 6].

A low resistivity was evidenced in the non-shadowed region, and a very high resistivity in the obstacle shadow region. The resistivity increases from $3 \cdot 10^{-4}$ Ω·cm to $2 \cdot 10^{3}$ Ω·cm for In_2O_3 films and from $6 \cdot 10^{-3}$ Ω·cm to 0.6 Ω·cm for ZnO films.

In order to check that the film smaller thickness is not responsible for the increase of the resistivity, very thin In_2O_3 and ZnO films (30-50 nm) were grown without obstacle at the same pressure of $1.3 \cdot 10^{-2}$ mbar and also at higher oxygen pressure (up to $2 \cdot 10^{-2}$ mbar) [5]. The resistivity of the In_2O_3 films grown without obstacle at $1.3 \cdot 10^{-2}$ mbar oxygen (the same pressure as in the obstacle case) was smaller when the film thickness was in the order of tens of nm compared to the 400 nm films ($6 \cdot 10^{-4}$ Ω·cm vs. $\sim 10^{-3}$ Ω·cm) . Such a dependence of the resistivity on the film thickness for In_2O_3 confirms that the origin of the very thin In_2O_3 films conductivity is mainly in the defects at the film surface, as reported in [14]. Therefore, the thickness dependence does not explain the high resistivity obtained behind the obstacle.

On the other hand, for ZnO films grown in the same conditions [6], a 100 nm film has a resistivity of $2.5 \cdot 10^{-2}$ Ω·cm, ~4 times greater than the value of $6 \cdot 10^{-3}$ Ω·cm obtained for the 400 nm film. However, this will still not explain the 100 times increase of the resistivity for ZnO films in the presence of the obstacle.

A possible explanation for the resistivity increase of the films grown behind the obstacle could be given by a reduction of the concentration of oxygen vacancies in that film region [5, 6]. The flux of the ablation plasma is reduced behind the obstacle compared to the adjacent regions, while the density of the oxygen remains the same. It has been previously shown in [15] that there is a larger percent of the ambient oxygen incorporated in the film when the ratio between the oxygen flux and ablated species flux is higher. Hence, due to the smaller plasma density behind the obstacle, there is a larger percent of oxygen incorporated in the film from the working gas, leading to a smaller density of oxygen vacancies in that region, and thus to a higher film resistivity.

The role of the surrounding oxygen density in the higher resistivity is confirmed by experiments

without obstacle at higher oxygen pressure. For In_2O_3 films grown at $2 \cdot 10^{-2}$ mbar the resistivity is several orders of magnitude greater, as well as for ZnO films grown at pressures above $1.5 \cdot 10^{-2}$ mbar.

Based on these results, self-assembled source-channel-drain structures for transparent thin film transistors were produced using the PED method in a single deposition process, by downscaling the obstacle geometry to a 300 μm diameter wire placed at 100 μm distance from the substrate [5].

4. CONCLUSIONS

The role of the obstacle inserted in the ablation plasma was studied by ion probe and its effect on the In_2O_3 and ZnO films by resistivity measurements. A slightly smaller mean ion energy (35 eV vs. 37.5 eV) and 16 times smaller total number of ions reaching the probe were observed behind the obstacle, which correlate with the 40 times smaller film thickness measured by profilometry under obstacle. The film resistivity increases by orders of magnitude behind the obstacle, and it has been proved that this effect is due to the additional incorporation of the oxygen from the working gas, and not to the smaller thickness of the film. The resistivity increase is less prominent for ZnO films grown with obstacle than that obtained for In_2O_3 films. These results show that the tuning of the electrical and optical properties in a single oxide film is possible for future applications in transparent electronics.

REFERENCES

[1] K. Nomura, H. Ohta, A. Takagi, T. Kamiya, M. Hirano and H. Hosono, "Room-temperature fabrication of transparent flexible thin-film transistors using amorphous oxide semiconductors", Nature, **432**, 488, 2004.

[2] R. L. Hoffman, B. J. Norris and J. F. Wager, "ZnO-based transparent thin-film transistors", Appl. Phys. Lett. **82** (5), 733, 2003.

[3] E M C Fortunato, P M C Barquinha, A C M B G Pimentel, A M F Goncalves, A J S Marques, R F P Martins and L M N Pereira, "Wide-bandgap high-mobility ZnO thin-film transistors produced at room temperature", Appl. Phys. Lett., **85**(13), 2541, 2004

[4] P.F.Carcia, "Application of Transparent Oxide Semiconductors for Flexible Electronics", in *Transparent Electronics: From Synthesis to Applications* Ed. By A.Facchetti ans T.Marks, Wiley & Sons Ltd , ISBN: 978-0-470-99077-3, 2010

[5] F. Gherendi, M. Nistor, S. Antohe, L. Ion, I. Enculescu, N.B. Mandache, "Self-assembled homojunction In_2O_3 transparent thin film transistors", Semicond. Sci. Technol. **28**(8) 085002, 2013.

[6] F. Gherendi, "The influence of an obstacle placed in the ablation plasma on the properties of oxide thin films", J. Optoel. Adv. Mater. **15**, (11-12), 1463-1469, 2013.

[7] M. Nistor, N.B. Mandache, J. Perrière, "Pulsed electron beam deposition of oxide thin films", J. Phys. D: Appl. Phys., **41** (16), 165205, 2008.

[8].S Tricot, Chantal Leborgne, M Nistor, E Millon and J Perriere, "Dynamics of a pulsed-electron beam induced-plasma: application to the growth of zinc oxide thin films", J. Phys. D: Appl. Phys. **41**, 175205, 2008

[9] S. Tricot, M. Nistor, E. Millon, C. Boulmer-Leborgne, N. B. Mandache, J. Perrière, W. Seiler, "Epitaxial ZnO thin films grown by pulsed electron beam deposition", Surf. Sci. **604**(21-22), 2024, 2010.

[10] W. Seiler, M. Nistor, C. Hebert, J. Perrière, "Epitaxial undoped indium oxide thin films: Structural and physical properties", Sol. Energ. Mat. Sol. Cells **116**, 34, 2013

[11] A. Marcu, C. Grigoriu, W. Jiang, K. Yatsui, "Pulsed laser deposition of YBCO thin films in a shadow mask configuration" Thin Solid Films **360** (1-2), 166, 2000.

[12] M. Nistor, F. Gherendi, N.B. Mandache, "The influence of an auxiliary discharge on the ablation plasma produced by a pulsed electron beam", J. Optoel. Adv. Mater., **10**, 2020-2023, 2008.

[13] Franz Gerhard, *Low Pressure Plasmas and Microstructuring Technology*, Springer-Verlag Berlin Heidelberg, ISBN 978-3-540-85849-2, 2009.

[14] S. Lany, A. Zakutayev, T.O. Mason, J.F. Wager, K.R. Poeppelmeier, J.D. Perkins, J.J. Berry, D.S. Ginley and A. Zunger, "Surface Origin of High Conductivities in Undoped Thin Films", Phys. Rev. Lett. **108** (1), 2–6, 2012.

[15] R. Gomez-San Roman, R. Pérez Casero, C. Maréchal, J.P Enard and J. Perrière, "^{18}O isotopic tracer studies of the laser ablation of $Bi_2Sr_2Ca_1Cu_2O_8$" J. Appl. Phys., **80** (3), 1787-1793, 1996.